

03

Influence of the diaphragm material at the entrance to the supersonic shock tube nozzle on the flow around a blunt body

© N.A. Monakhov, P.A. Popov, V.A. Sakharov, S.A. Poniaev, R.P. Kurakin

Ioffe Institute,
194021 St. Petersburg, Russia
e-mail: nikolay.monakhov@mail.ioffe.ru

Received February 25, 2024

Revised February 27, 2024

Accepted February 27, 2024

The results of experiments on measuring pressure and heat flow near the critical point of a blunt body in experiments on a shock tube with a nozzle are presented. It is shown that fragments of the diaphragm at the nozzle inlet have a significant effect on the flow structure near the critical point of the model and distort the signals of pressure and heat flow sensors. A method has been proposed to significantly improve the quality of a high-speed flow by selecting the optimal material and thickness of the diaphragms at the entrance to the supersonic nozzle.

Keywords: shock tube, high-speed flow, diaphragm rupture, heat flux measurement.

DOI: 10.61011/JTF.2024.04.57528.49-24

Introduction

Generally, an experimental study of high enthalpy flow over models is carried out at pulse-action gasdynamic facilities, such as a shock tunnel [1,2] with a nozzle at the end. Such facilities feature availability of a diaphragm that separate the nozzle inlet and the shock tunnel's driven section. After the shock wave reflection from the tunnel end the diaphragm is destructed, after which its fragments are involved into the flow. The presence of solid particles in the gas flow disturbs the shock wave pattern near to the model in the flow [3,4] and distorts readings of sensors on its surface, which results in decrease of the duration of quasi-steady-state flow over of the models under study and in a significant deviation of gas-dynamic parameters of the high-speed flow from the expected ones [5–9]. The results of numerical simulation of the flow in the shock layer under impact of high inertia particles show that when relatively coarse particles collide with a body in the flow, these are reflected and next move against the supersonic flow. Such a movement is accompanied by the destruction of a stationary shock wave structure and formation of a cone-shaped disturbed region with the apex moving along with the particle, as well as formation of an impact annular jet directed towards the surface of the body in the flow and interacting with it, with the creation of a high-pressure and convective heat transfer region [10–14]. Lower-size particles, due to their low inertia, move along with the flow and do not cause a significant impact on the flow structure recorded by means of a Schlieren diagnostics. Their presence is manifested as a high-frequency noise in the signals of pressure transducers, without impact on the mean value of the measured pressure.

An additional problem related to the presence of solid particles in the flow refers to mechanical damage of the surface of sensitive elements of the sensors located on the

model surface, which, finally, results in their destruction. Basically, this problem concerns heat flux measurements, because the surface of heat sensors must be in direct contact with the oncoming gas flow [7]. At the present time, thin-film resistance sensors [15] and various thermoelectric sensors based on thin films with artificial anisotropy [16,17], coaxial thermocouples [7], and anisotropic thermoelements made of bismuth and heterogeneous metallic structures are used for the measurement of heat flows at the pulse-action gas-dynamic facilities [18,19]. Thermal sensors based on thin films are the mostly subjected to the impact of solid particles in a high-speed flow created in the shock tunnel. In fact, such sensors withstand only one experiment. Coaxial thermocouples have a higher mechanical strength, however, impact of solid particles on the work surface of a coaxial thermocouple gradually leads to failure of contact within the soldering area and to destruction of the sensor itself [7].

The purpose of this study is to find approaches that would contribute into the reduction of the diaphragm fragments number formed in case of its destruction, and into the improvement of the high-speed flow quality. Material and thickness of the diaphragm at the inlet into the supersonic nozzle were selected. Since it is not possible to completely remove the diaphragm fragments from the gas flow, creation of materials and heat sensor designs having a higher mechanical strength, and the flow quality control by measuring pressure and heat flux near to the critical point of the model in the flow and based on the shady flow patterns obtained seems to be relevant as well.

1. Heat flux sensor based on metallic heterogeneous structures

The own experience in measurements of heat flux in shock tunnels shows that heat sensors based on anisotropic

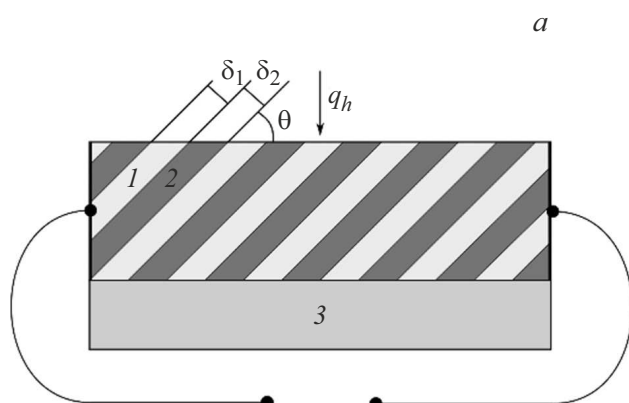


Figure 1. Internal structure of sensitive element of heterogeneous gradient heat flux sensor (*a*) and appearance of the sensor used in the insert (*b*).

materials (crystalline bismuth and metallic heterogeneous structure) are the most convenient for the application in experiments and resistant to mechanical impacts. A bismuth-based heat sensor is a battery of 10–20 serially connected thermoelements laid onto a substrate made of mica [18,19]. Such a number of soldered joints increases the risk of failure of contact as a result of impact on the sensor by the flow with solid particles. A heat sensor based on metallic heterogeneous structures (heterogeneous gradient heat flux sensor (HGHFS)) used herein has no such disadvantages.

A sensitive element of HGHFS is a plate of alternating layers of different metals 1 and 2 with the thickness of δ_1 and δ_2 oriented towards the work surface at the angle of θ (Fig. 1, *a*) and having different Seebeck coefficients. The layers are interconnected by means of diffusion welding. The plate is attached onto electric insulating substrate 3. Wires for electric signal registration are soldered to side faces. The pairs of metals having as different as maximum Seebeck coefficients are used to manufacture a sensitive element: chromel–alumel, copper–nickel, steel–nickel, etc. [18]. The operating principle of HGHFS is based on generation of thermoelectrical field within the structure with thermo-emf anisotropy when the temperature gradient occurs [20]. The expected level of volt-watt coefficient of such sensors is 10–20 $\mu\text{V}/\text{W}$ and is determined by the density, thermal conductivity and Seebeck coefficient of the pair of metals used for its manufacture, as well as by the number of layers and their thickness [21]. In this case the sensor signal level under impact of heat flux with the typical density for gas-dynamic experiment in shock tunnels of $\sim 1 \text{ MW}/\text{m}^2$ does not exceed 100 μV . For that reason a device with the amplification factor of at least 100 is used for registration of signal of such sensors.

For HGHFS calibration and using it for measurement of heat flux in the pulse gas-dynamic experiment, often it is need to install the sensor on the surface of various models in the flow and in channels of shock tunnels. A removable metallic insert of special design was developed for that

purpose (Fig. 1, *b*). Full length of the insert including the connector was 47 mm, of which the body itself — 31 mm, the diameter — 14 mm. Prior to installation of the sensor into the insert, all surfaces within the volume of seats were prepared by grinding and polishing, then the volume of seats was filled with a binder. Dual-component epoxy glue of Poxipol brand, and acrylic acid were tested as different options of the binder. In the case of acrylic acid, the seat volume was subjected to additional heat treatment by exposure to laser for crystallization of amorphous structure of the binder. Preliminary tests in the shock tunnel demonstrated a higher resistance of the sensor to heavy mechanical and erosion impact from the high-speed flow, when acrylic acid was used as a binder. For that reason all experimental results given below were obtained with this method of HGHFS attachment on the insert.

2. Experimental setup description

Large shock tunnel of the Ioffe Institute [22] is a tool for generation of high-speed flows having a quite wide range of basic parameters (density, pressure, temperature). The setup layout is shown in Fig. 2. The length of the driver section is 3.3 m, the length of the driven section — 12.4 m. The inside cross-section diameter of the shock tunnel is — 100 mm.

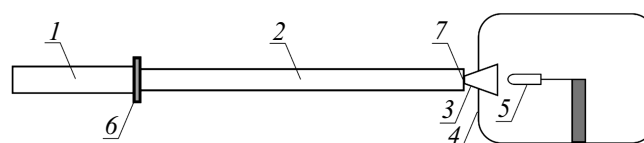


Figure 2. Layout of the Large Shock Tunnel of the Ioffe Institute: driver section (1) and driven section (2), supersonic nozzle (3), damper tank (4), model under study (5), metallic diaphragm (6), diaphragm at the inlet into supersonic nozzle (7).

The shock wave speed was measured using a basic method by means of two piezoelectric pressure transducers designed by G.N. Suntsov, installed in the driven section flush with the inside surface of the shock tunnel at the distance of 230 mm from each other. The uncertainty of measured shock speed did not exceed 3%.

Conical supersonic nozzle connected to the damper tank is installed in the end of the shock tunnel driven section. The nozzle semiapex angle is 11° , and the throat diameter is 10 mm, relative expansion is 100.

The gas parameters behind the reflected shock wave and near to the model surface were calculated based on the initial conditions of the experiment (initial nitrogen pressure in the driven section and Mach number of primary shock wave). Equilibrium gas parameters behind the reflected shock wave were calculated subject to real gas properties at high temperatures. The flow parameters at the nozzle outlet were calculated by using 1D model subject to the final rate of chemical reactions.

Hemispherical model with the diameter of 70 mm was made of ABS-plastic by 3D-printing. Such a manufacturing method is conditioned by a complex model topology due to the need for the sensors attachment inside the model and their access to its surface. The model was attached inside the damper tank along the nozzle axis at the distance of 30 mm from its outlet. Such position of the model provided the convenience of Schlieren diagnostics of the flow over in the experiment. The total pressure near to the stagnation point of the model was measured by means of PCB piezoelectric sensor of the model 113B28 with the sensitivity of 15.6 mV/kPa and time resolution of at least $2\mu\text{s}$. The pressure transducer was installed inside the model and connected with its surface via cylindrical channel with the diameter of 2 mm and the length of 5 mm to protect it against damages by diaphragm fragments. The pressure transducer and heat flux sensor signals were registered by means of Tektronix TDS 1002 oscilloscopes with the time resolution of $1\mu\text{s}$.

HGHFS heat sensor with the plan size of 3×3 mm and the thickness of 0.5 mm was composed of 9 layers of copper and 9 layers of nickel and was installed in the insert (Fig. 1, *b*). The sensor was connected to the amplifier assembled on the basis of INA128 microcircuit with the amplification factor 216, installed inside the model. The amplifier's bandwidth of ~ 200 kHz provides the time resolution of the „sensor+amplifier“ pair of at least $5\mu\text{s}$, which is sufficient to measure heat flux in gas-dynamic experiments with specific duration of ~ 1 ms. Within the framework of 1D thermoelectrical model of the sensor the electric signal is proportional to the difference of temperatures between its working and rear surfaces. Calculation of heat flux based on the electric signal of the sensor was performed according to the procedure [23], which is based on iterative resolution of 1D equation of thermal conductivity. For the purpose of protection against electromagnetic interferences of the heat flux sensor signal, the registration channel was powered from a battery.

Before using this sensor in the experiments with high speed flow over a model, it was calibrated by using the procedure based on the gas heating process behind the reflected shock wave [24]. Because of the specifics of the Large Shock Tunnel of the Ioffe Institute, the measurement behind the reflected shock wave requires significant modification of its nozzle unit. For that reason, the calibration thermal measurements were performed at a Small Shock Tunnel of the Ioffe Institute [19,24,25] with the inside cross section diameter of 50 mm. The small shock tunnel was equipped with a fast acting valve that ensures the start of the shock wave process in the tunnel at a known pressure in its driver section. Such an approach provided the flow behind the reflected shock wave with quite accurately predictable gas-dynamic parameters, which was the necessary pre-requisite for the measurement of the HGHFS calibration factor with the required accuracy.

In 1D approach, with no gas dissociation and ionization, and the power-law relation of the gas thermal conductivity and density on the temperature, the heat flux towards the end wall behind the shock wave with reflection of the shock wave depends on the time $q(t) \propto t^{-1/2}$ as [26]. Theoretical and experimental values of the standardized heat flux $q \cdot \sqrt{t}$ depending only on the gas parameters behind the reflected shock wave are compared. According to the results of these two experiments, the volt-watt coefficient of HGHFS S_0 was $15\mu\text{V/W}$.

Visualization of Schlieren patterns of the model flow over was performed by means of the IAB-451 Schlieren device. Semiconductor laser with the pulse duration of about 10 ns was used as a backlight source. The Schlieren pattern was registered by a digital photo camera. Synchronization of all measuring instruments, as well as of drive pulse for the semiconductor laser was provided by the signal of piezoelectric pressure transducer located in the measuring section of the shock tunnel at the distance of 1080 mm from nozzle inlet.

Before the beginning of experiments the shock tunnel sections were separated from each other by a metallic diaphragm with cross-shaped notch. Metallic diaphragm rupture occurred upon reaching the required pressure in the driver section. Thin diaphragm was installed at the nozzle inlet, whose rupture at the moment of the shock wave reflection from the tunnel end triggered the start of gas-dynamic process in the nozzle. Herein we experimentally studied the features of high-speed flow over the model when using different diaphragms at the nozzle inlet. We used Mylar diaphragms with the thickness of $80\mu\text{m}$, as well as polyethylene diaphragms with the thickness of 5 and $10\mu\text{m}$.

3. Results

At the present time, the study of high-enthalpy flows simulating the aerodynamics of a high-speed flight in various atmospheres is of the highest interest. A series of preliminary experiments was performed to study the maximum capabilities of HGHFS for thermal measurements during

Statistics of the experiments with the use of Mylar diaphragms in terms of the presence of the flow artefacts on the registered shady patterns

P_1 , mbar	Quantity experiments	Without artefacts Schlieren pattern	With artefacts Schlieren pattern	Percentage experiments without artefacts Schlieren pattern
0–40	23	22	1	96
41–100	11	6	5	55
101–300	31	16	15	52
301–800	23	8	15	35

high-speed flow over with high stagnation temperatures. It appeared that the pulse load of the flow at the stagnation temperature of ~ 5000 K did not lead to the sensor destruction or to a significant change of its properties even after the series of 10 experiments, which is a good value versus the crystalline bismuth-based sensors. At a higher stagnation temperature ~ 6000 K „the sensor lifetime“ on the model did not exceed 1–2 experiments, which should be treated at the moment as the top limit of the stagnation temperature range, at which the use of HGHS is allowed for thermal measurements. In such experiments the sensor was torn off by the flow from the model surface, which, apparently, was caused by destruction of acrylic base that connects the sensor with the model surface, due to occurring temperature gradient.

The surface of sensitive element of the sensor is being contaminated during flow over and, rigorously speaking, its cleaning is required prior to every experiment, however, repeated calibration of the sensor according to the procedure [24] has shown stability of its volt-watt coefficient $S_0 = 15 \mu\text{V/W}$.

In the series of more than 80 experiments for the hemispherical model flow over it was found that, when using Mylar diaphragms, disturbances of the bow shock wave occur in some cases on the Schlieren patterns near to the model's critical point. These disturbances occurred in a probabilistic nature. The analysis has shown that these disturbances do not occur, if the initial pressure in the shock tunnel driver section does not exceed 40 mbar, in all other cases these disturbances appear with some frequency, wherein the frequency of appearance increases as far as the pressure increases. A small additional series of experiments was carried out at other nozzles enabling creation of the flow with different Mach numbers. In this case the disturbances on Schlieren patterns of flow over appeared in single experiments only.

Table provides statistical data on the frequency of occurrence of such disturbances depending on the initial conditions of the gas-dynamic experiment.

The analysis of references has shown that such effect was also observed many times before [5,6,9], and it is caused by the presence of solid particles different in size in the high-speed flow, which are formed in case of destruction of

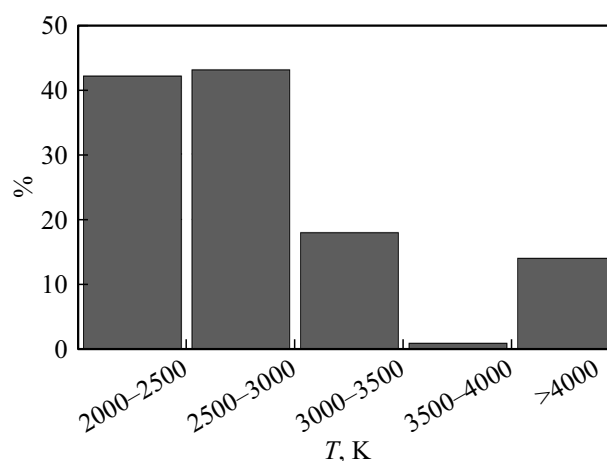


Figure 3. Dependence of the frequency of occurrence of the bow shock wave disturbances on the gas stagnation temperature.

Mylar diaphragm at the supersonic nozzle inlet. Abrupt increase of the pressure at the moment of shock wave coming leads to formation of a high number of diaphragm fragments due to Mylar fragility under pressure load. The paper [27] studied the process of destruction of cellophane diaphragm separating the driver and driven sections of the shock tunnel. It was established that the destruction process starts at the maximum tension point and is accompanied by formation of both coarse and fine fragments. Since Mylar has similar to cellophane mechanical characteristics, one should expect a similarity of the destruction process of diaphragms made of these materials.

Fig. 3 shows the dependence of occurrence of the bow shock wave disturbances during flow over a hemisphere on the flow stagnation temperature. More rare occurrence of disturbances of Schlieren pattern of flow over at $P_1 < 40$ mbar and at other nozzles is caused by the specifics of the membrane destruction (formation of fine particles) at a higher gas temperature at the nozzle inlet, as well as by the change of their flying time and impossibility of their visualization.

Fig. 4 shows typical Schlieren patterns of flow over models with disturbance of the shock wave structure caused by single particle (Fig. 4, a) and several particles

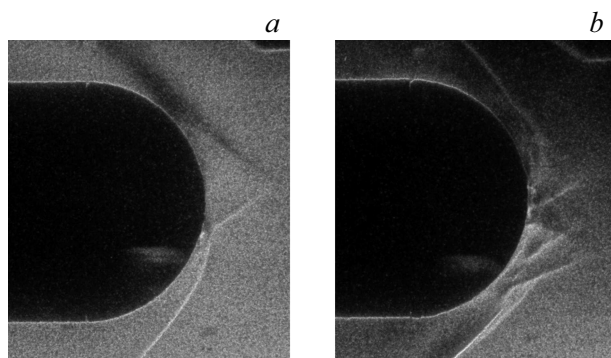


Figure 4. Schlieren image of flow over a blunt body with disturbance caused by single particle (a) and several particles (b).

(Fig. 4, b). The patterns were obtained at the time instant of $t = 1$ ms from the moment of primary shock wave coming to the nozzle inlet and the start of the diaphragm destruction at the nozzle inlet. It should be noted that determining of the duration of the stationary shock-wave structure disturbance by analysis of the results of single-frame Schlieren diagnostics is impossible. However, such shock-wave pattern variation impacts on the gas-dynamic parameters of the flow near to the stagnation point of the model and could be registered, for example, by measuring the pressure and the heat flux at the surface of the model surface.

Fig. 5 shows signals of the pressure transducer (Fig. 5, a) and heat flux sensor (Fig. 5, b) at the stagnation point of the model during supersonic flow over containing solid particles of Mylar diaphragm. High-frequency component will appear within the signal spectrum of the pressure transducer (Fig. 5, a). Such a component with the frequency of ~ 100 kHz is present virtually in all experiments. In a series of cases the amplitude of high-frequency oscillations

rises significantly. This allows to assume that their occurrence is associated with excitation of natural oscillations of the pressure transducer. The question about the role of solid particles in occurrence of such component within the signal spectrum of the pressure transducer and about its amplitude dynamics remains open. Wherein, average level of the pressure transducer signal remains corresponding to the expected stagnation pressure. As shown by the analysis of the measurement results, occurrence of relatively long „dips“ of the pressure transducer signal (about $t = 0.8$ ms) is caused by solid particles, namely, the fault in the shock-wave structure of the bow wave caused by them.

The heat flux sensor signal (Fig. 5, b), which is proportional to the temperature differences at the top and rear surfaces of the heat flux sensor sensitive element remains smooth throughout the registration time. The difference from the pressure transducer signal reviewed above is caused by considerably higher inertia of the heat transfer processes in the gas and in the sensitive element of the sensor. The practical interest is about the value of the heat flux towards the model surface, which is calculated by using the procedure [21]. Fig. 6 shows comparison of change of the pressure and heat flux at the model's stagnation point. The plot shows a strict time correlation of change of the pressure and heat flux at the stagnation point.

Oscillations of the measured values are observed, whose level for the pressure reaches that of the pressure itself, and for the heat flux could exceed it several times. Such a behavior of the pressure and of the heat flux qualitatively correlates the results of numeric simulation of movement of coarse particles in the shock layer in the full-scale 3D setup based on the mesh-free method of resolution of a system of equations for gas dynamics [10–114]. Reaching a quantitative match of the results of calculation and of the experiment seems to be impossible due to inability to

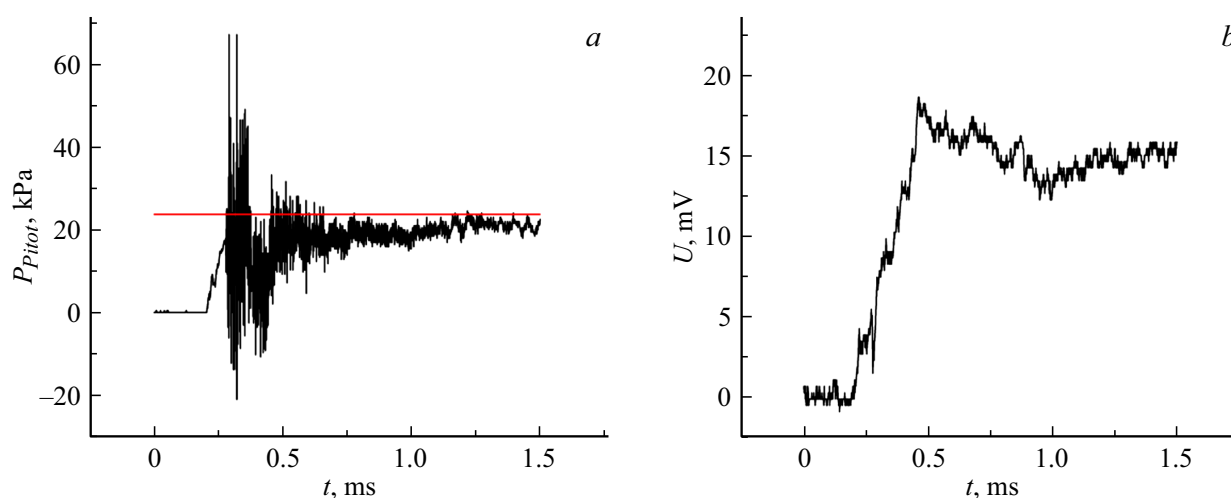


Figure 5. Impact of solid particles of Mylar diaphragm on the pressure transducer (a) and heat flux sensor signals (b). The flow Mach number $M = 6.1$, the pressure of 0.65 kPa, and the temperature of 492 K. Red horizontal line refers to the stagnation pressure at the critical point calculated by using the 1D model.

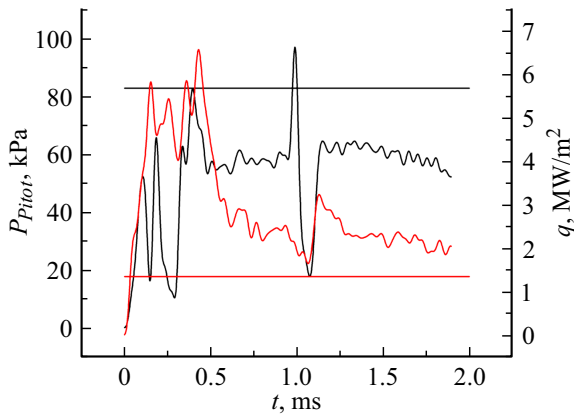


Figure 6. Measured pressure (black curve) and heat flux (red curve). The black horizontal line shows stagnation pressure at the stagnation point calculated by using 1D model, the red one — is the heat flux in case of undisturbed flow over, calculated by using the Fay–Riddell theory [28]. The flow Mach number $M = 6.6$, the pressure of 1.37 kPa, and the temperature of 304 K.

control the diaphragm rupture process at the nozzle inlet and the absence of information about the quantity and sizes of diaphragm fragments formed during the rupture.

Therefore, when using Mylar diaphragm at the nozzle inlet, heavy impact of its fragments in the flow on the current is observed near to the stagnation point. The importance of this problem rises subject to a limited test time of pulsed gasdynamic facility operation, because typical duration of dips in the pressure transducer signal could be hundreds of microseconds with the total time of existence of the quasi-steady-state flow over with the required parameters not exceeding 1 ms. For that reason, a search for engineering solutions contributing into the resolution of that issue is required. One of possible ways of resolution is the use of diaphragms made of the other material. Herein we used polyethylene diaphragms with the thicknesses of 5 and 10 μm . Selection of polyethylene as an alternative for Mylar is

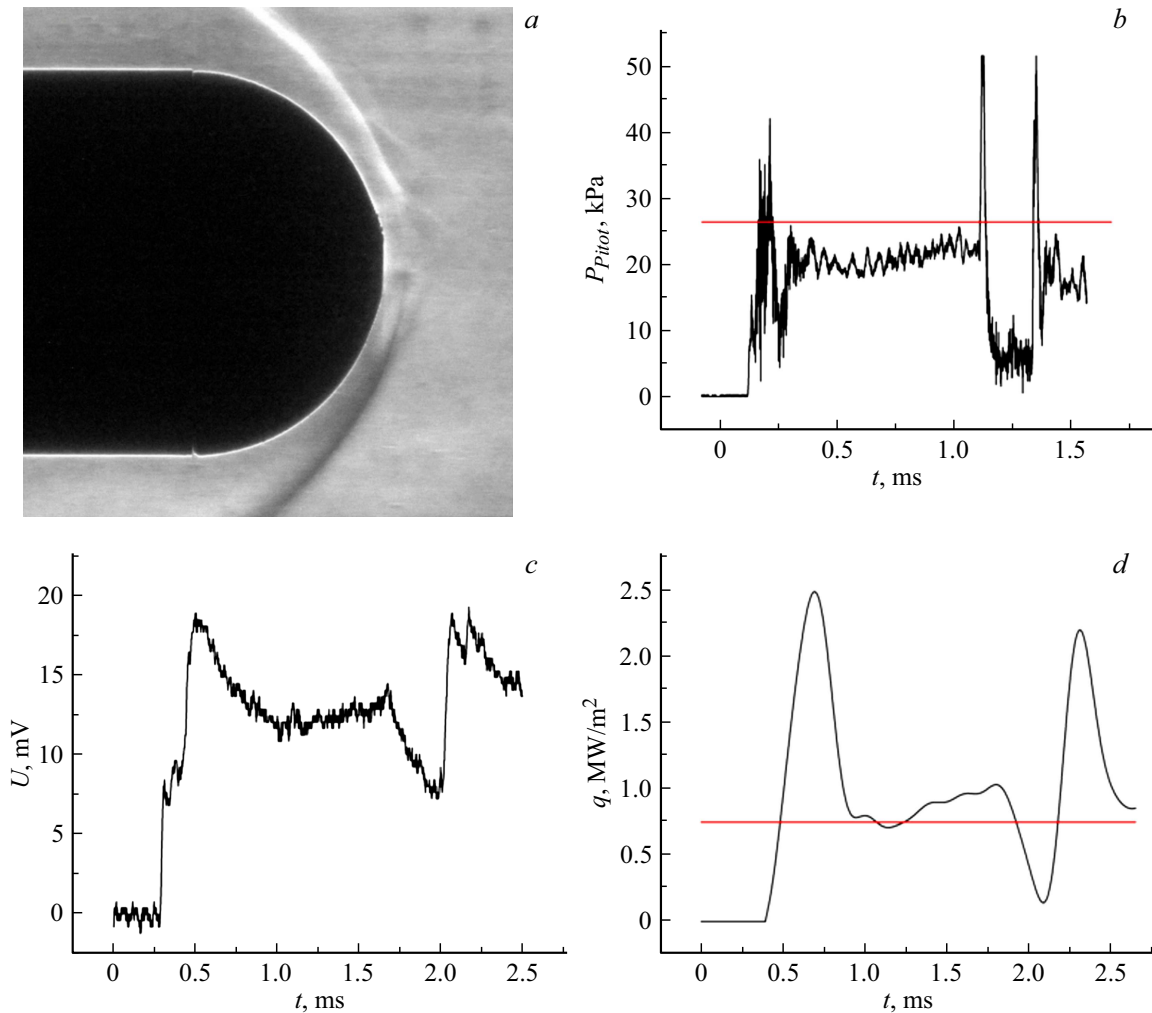


Figure 7. Results of the study of the flow over blunt body when using polyethylene diaphragm with the thickness of 5 μm ; *a* — Schlieren pattern of flow over at the moment of time $t = 1$ ms from the start of the diaphragm destruction at the nozzle inlet; *b* — pressure measured near to the stagnation point of the model; *c* — HGHS signal; *d* — heat flux at the stagnation point of the model obtained by means of HGHS signal processing. The Mach number $M = 6.4$, the pressure of 0.51 kPa, and the temperature of 310 K. Red horizontal lines refer to the stagnation pressure at the stagnation point calculated by using 1D model and heat flux calculated by using Fay–Riddell theory [28].

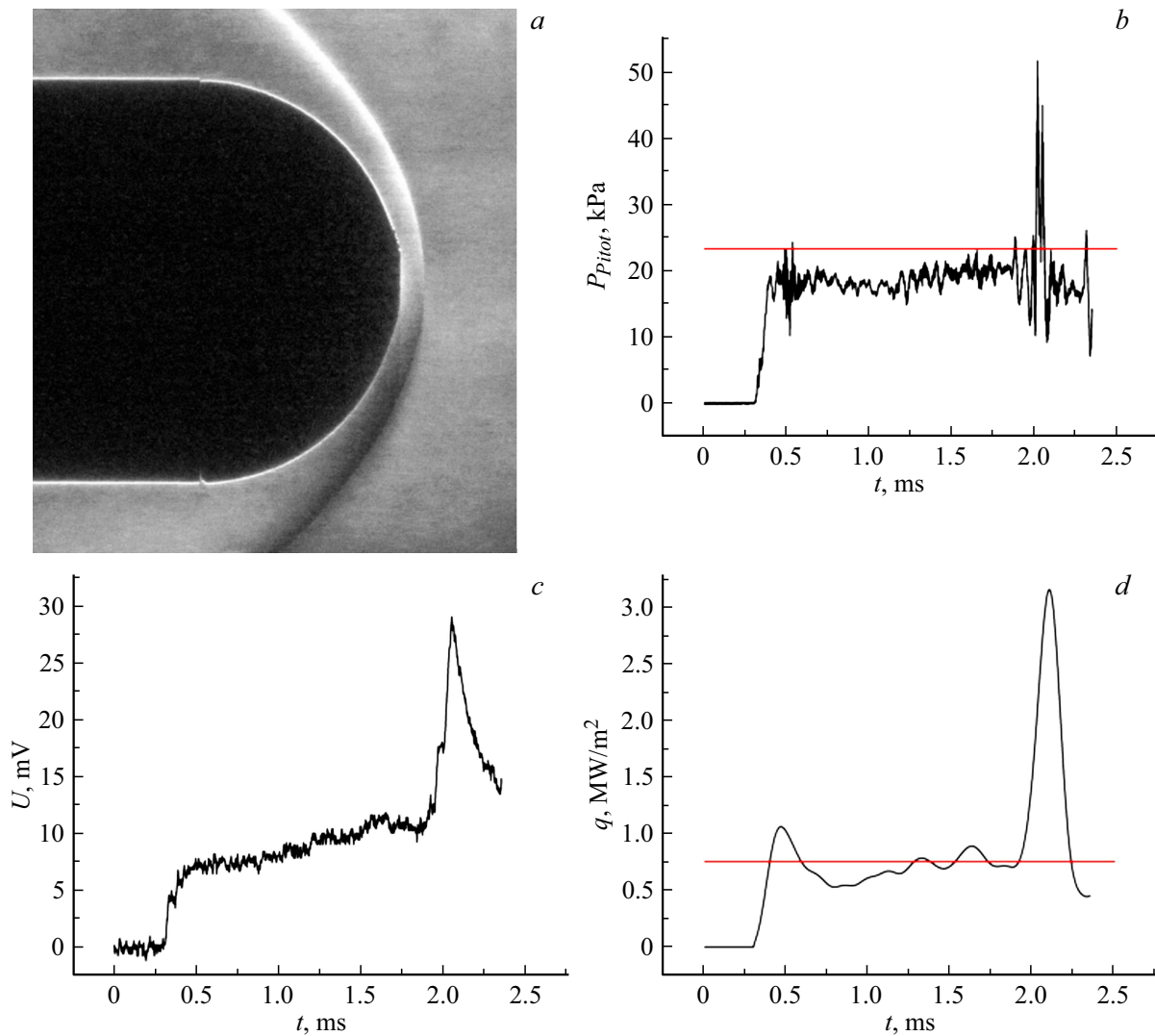


Figure 8. Results of the study of the flow over blunt body when using polyethylene diaphragm with the thickness of $10\ \mu\text{m}$; *a* — Schlieren pattern of flow over at the moment of time $t = 1\ \text{ms}$ from the start of the diaphragm destruction at the nozzle inlet; *b* — pressure measured near to the stagnation point of the model; *c* — HGHS signal; *d* — heat flux at the stagnation point of the model obtained by means of HGHS signal processing. The Mach number $M = 6.4$, the pressure of $0.49\ \text{kPa}$, and the temperature of $304\ \text{K}$. Red horizontal lines refer to the stagnation pressure at the stagnation point calculated by using 1D model and heat flux calculated by using Fay–Riddell theory [28].

caused by its higher elasticity — the polyethylene film fragmentation occurs with formation of lower number of fragments versus the Mylar diaphragm. As a consequence, the probability of coarse diaphragm fragments ingress into the high-speed flow and distortion of the shock-wave pattern of the model flow over is significantly reduced.

Fig. 7 shows the results of the study of the flow over blunt body when using polyethylene diaphragm with the thickness of $5\ \mu\text{m}$. In Fig. 7 one can note small disturbances of the bow shock front. The pressure change at the model surface corresponding to them is represented as a dip with the duration of about $150\ \mu\text{s}$ within the region $t = 1000\ \mu\text{s}$ in Fig. 7, *b*. Wherein, average pressure level during test time process is in a good correlation with the calculation by

using 1D model. The same as in the case of using Mylar diaphragm (Fig. 6), the impact of polyethylene diaphragm fragments on the flow structure leads to simultaneous abrupt changes in pressure (Fig. 7, *b*) and heat flux (Fig. 7, *d*). The amplitudes of these changes are comparable to undisturbed values of such parameters that correspond to the area of quasi-steady-state flow over the model.

Fig. 8 shows the results of the study of flow over blunt body when using a thicker polyethylene diaphragm with the thickness of $10\ \mu\text{m}$. It can be seen from the Schlieren pattern (Fig. 8, *a*) that the bow shock wave front is smooth. Relative level of the pressure transducer signal oscillations (Fig. 8, *b*) does not exceed 20%, wherein the pressure constancy is observed throughout the shock tunnel test time ($1\ \text{ms} < t < 2\ \text{ms}$). A small (not to exceed 15%) difference

of the experimental level of pressure from the one predicted by the 1D calculation, apparently, is caused by the error of determination of the gas parameters at the supersonic nozzle inlet, as well as by the viscosity impact on the flow in the nozzle. Local heat flux maximum (Fig. 8, *d*) caused by the start shock wave coming to the blunt body, in case of using a thick polyethylene diaphragm is much lower than when using a polyethylene diaphragm with the thickness of $5\ \mu\text{m}$ (Fig. 7, *d*). It is caused by no ingress of coarse fragments of the diaphragm into the flow region near to the stagnation point of the blunt body.

Conclusion

The experiments have shown that Mylar diaphragms installed within the critical section of the shock tunnel's supersonic nozzle are destructed with formation of fragments of different sizes. Schlieren images, as well as measurement of pressure and heat flux at the stagnation point of blunt body have shown that their presence in the gas flow could lead to occurrence of gas-dynamic disturbances near to the blunt body. It was established that coarse fragments of diaphragms, when reflected from a blunt body surface, significantly distort the flow over shock-wave pattern and the readings of pressure transducers and heat flux sensors. It is shown that increase of gas temperature behind the reflected shock wave at the nozzle inlet reduces the probability of disturbances occurrence. Fine fragments of diaphragms lead to occurrence of a high-frequency noise in the pressure transducer readings, without changing the average level of its signal.

Use of polyethylene diaphragms because of their higher elasticity allows to reduce the number of diaphragm fragments entering the flow. It was established that destruction of polyethylene diaphragms with the thickness of $5\ \mu\text{m}$ is similar to Mylar and is accompanied by formation of fragments with different sizes that impact the gas-dynamic flow over pattern. Destruction of polyethylene diaphragm with the thickness of $10\ \mu\text{m}$ leads to formation of fine fragments, whose interaction with a working gas heated by the reflected shock wave does not lead to a considerable impact on the high-frequency component of the pressure transducer signal. At that, the quality of high-speed flow is improved significantly, which is also confirmed by the results of the Schlieren diagnostics and measurement of heat flux near to the blunt body stagnation point.

Conflict of interest

The authors declare that they have no conflict of interest.

References

- [1] P. Reynier. *Progr. Aerospace Sci.*, **85**, 1 (2016). DOI: 10.1016/J.PAEROSCI.2016.04.002

- [2] V.A. Miller, M. Gamba, M.G. Mungal, R.K. Hanson. *AIAA J.*, **52** (2), 451 (2014). DOI: 10.2514/1.J052767
- [3] A.A. Verevkin, Yu.M. Tsirkunov. *J. Appl. Mech. Tech.*, **49** (5), 789 (2008). DOI: 10.1007/s10808-008-0099-y
- [4] S.V. Panfilov, D.A. Romanyuk, Y.M. Tsirkunov. *Fluid Dyn.*, **58** (4), 569 (2023). DOI: 10.1134/S0015462823600487
- [5] K.K.N. Anbuselvan, K.P.J. Reddy. *AIAA J.*, **55** (10), 3603 (2017). DOI: 10.2514/1.J055523
- [6] S. Gu, H. Olivier. *Progr. Aerospace Sci.*, **113**, 100607 (2020). DOI: 10.1016/j.paerosci.2020.100607
- [7] Ch.M. James, B. Birch, D.R. Smith, T.G. Cullen, Th. Millard, S. Vella, Yu Liu, R.G. Morgan, N. Stern, D. Buttsworth. (AIAA Paper 2019–3007). *AIAA Aviation 2019 Forum*. DOI: 10.2514/6.2019-3007
- [8] W.A. Fleener, R.H. Watson. *AIAA Paper*, **73**, 761 (1973).
- [9] M.S. Holden, G.Q. Gustafson, G.R. Duryea, L. Hudack. *AIAA Paper*, **76**, 320 (1976).
- [10] D.L. Reviznikov, A.V. Sposobin, I.E. Ivanov. *High Temperature*, **56** (6), 884 (2018). DOI: 10.1134/S0018151X18050218
- [11] A.V. Sposobin, D.L. Reviznikov, I.E. Ivanov, I.A. Kryukov. *Izvestiya Vuzov. Aviatsonnaya tekhnika*, **4**, 108 (2020) (in Russian).
- [12] D.L. Reviznikov, A.V. Sposobin, I.E. Ivanov. *High Temperature*, **58** (6), 839 (2020). DOI: 10.1134/S0018151X20060164
- [13] V. Sposobin, D.L. Reviznikov. *Fluids*, **6** (11), 406 (2021). DOI: 10.3390/fluids6110406
- [14] A.V. Sposobin. *Trudy MAI*, **125**, 36 (2022) (in Russian).
- [15] T. Alam, R. Kumar. *Rev. Sci. Instrum.*, **92** (3), 031501 (2021). DOI: 10.1063/5.0015932
- [16] H. Knauss, T. Roediger, D.A. Bountin, B.V. Smorodsky, A.A. Maslov, J. Srulijes. *J. Spacecrafts and Rockets*, **46** (2), 255 (2009). DOI: 10.2514/1.32011
- [17] M.A. Kotov, A.N. Shemyakin, N.G. Solovyov, M.Y. Yakimov, V.N. Glebov, G.A. Dubrova, A.M. Malyutin, P.A. Popov, S.A. Poniaev, T.A. Lapushkina, N.A. Monakhov, V.A. Sakharov. *Appl. Therm. Eng.*, **195**, 117143 (2021). DOI: 10.1016/j.applthermaleng.2021.117143
- [18] S.Z. Sapozhnikov, V.Yu. Mityakov, A.V. Mityakov. *Heatmetry: The Science and Practice of Heat Flux Measurement: Heat and Mass Transfer* (Springer International Publishing, 2020)
- [19] P.A. Popov, N.A. Monakhov, T.A. Lapushkina, S.A. Poniaev. *ZhTF*, **92** (9), 1334 (2022) (in Russian). DOI: 10.21883/JTF.2022.09.52924.54-22
- [20] D.M. Rowe. *Thermoelectrics Handbook: Macro to Nano* (CRC Press, 2006)
- [21] P.A. Popov, N.A. Monakhov. *St. Petersburg Polytechnic University J. Phys. Mathematics*, **16** (1.1), 444 (2023).
- [22] V.G. Maslennikov, V.A. Sakharov. *Tech. Phys.*, **42** (11), 1322 (1997). DOI: 10.1134/1.1258870
- [23] P.A. Popov, S.V. Bobashev, B.I. Reznikov, V.A. Sakharov. *Tech. Phys. Lett.*, **44** (4), 316 (2018). DOI: 10.1134/S1063785018040235
- [24] P.A. Popov, N.A. Monakhov, T.A. Lapushkina, S.A. Poniaev, R.O. Kurakin. *Tech. Phys. Lett.*, **48** (10), 46 (2022). DOI: 10.21883/TPL.2022.10.54798.19297

- [25] S.V. Bobashev, A.V. Erofeev, T.A. Lapushkina, S.A. Poniaev, R.V. Vasil'eva, D.M. Van Wie. *J. Propuls. Power*, **21** (5), 831 (2005). DOI: 10.2514/1.2624
- [26] J.A. Fay, N.H. Kemp. *J. Fluid Mech.*, **21** (4), 659 (1965). DOI: 10.1017/S002211206500040X
- [27] G. Fukushima, T. Tamba, A. Iwakawa, A. Sasoh. *Shock Waves*, **30**, 545 (2020). DOI: 10.1007/s00193-020-00951-2
- [28] J.A. Fay, F.R. Riddell. *J. Aerosp. Sci.*, **5** (25), 73 (1958). DOI: 10.2514/8.7517

Translated by D.Kondaurov